

What can a relativistic quark model tell us about charmed mesons?

M. Sutherland^a, B. Holdom^b, S. Jaimungal^c and Randy Lewis^d

Department of Physics, University of Toronto
60 St. George St., Toronto, Ontario
Canada M5S 1A7

Abstract

A relativistic quark model is extended to incorporate chiral and gauge symmetries. We obtain the $DD^*\pi$ and $DD^*\gamma$ couplings and find that the ratio $\Gamma(D^{*0} \rightarrow D^0\pi^0)/\Gamma(D^{*0} \rightarrow D^0\gamma)$ constrains the charm-quark mass close to 1.45 GeV. Large $1/m_c$ corrections appear in the heavy-quark contribution to the $DD^*\gamma$ coupling. The model is extended further to describe seven excited D meson states. We find that semileptonic B decays into the ground and excited D meson states do not account for the total semileptonic decay width of the B^0 . The nonresonant contributions to the processes $\bar{B}^0 \rightarrow D^{(*)}\pi\ell\bar{\nu}$ appear to be large enough to account for the discrepancy.

^a marks@medb.physics.utoronto.ca

^b holdom@utcc.utoronto.ca

^c jaimung@physics.ubc.ca

^d lewis@oldkat.physics.utoronto.ca

Introduction

We have recently developed a fully relativistic model of hadrons containing one heavy quark [1]. Hadronic matrix elements are represented by quark loop graphs with momentum dependent interaction vertices between hadron, heavy quark and light quark. The only parameters in the model are the quark masses. We previously applied the model to $\bar{B} \rightarrow D^{(*)}\ell\bar{\nu}$ [2, 3], $\bar{B} \rightarrow K^*\gamma$ [4], $\Lambda_b \rightarrow \Lambda_c\ell\bar{\nu}$ [5], and $\Omega_b^{(*)} \rightarrow \Omega_c^{(*)}\ell\bar{\nu}$ [6]. The model does not rely on any expansion in inverse powers of heavy-quark masses m_Q . However, QCD imposes severe constraints on the form of the heavy-quark expansion, and not all models automatically satisfy these constraints [7]. We have verified that the heavy-quark expansion of our model does satisfy these constraints.

Confinement is modeled in a simple way; we simply drop the imaginary parts of our loop graphs. This prescription preserves the symmetry structure of the theory, and our hypothesis is that it may give reasonable results as long as external momenta of a diagram are such as to be far removed from whatever unphysical singularities the diagram possesses. (A discussion of the singularity structure of our three-point functions, including anomalous thresholds, may be found in [8].) We are finding that this simple, most naive model of confinement is yielding some very encouraging results. It also acts as a useful preview to the general Bethe-Salpeter approach.

Although our results are based only on a model, they suggest that some caution is required in the use of more systematic attempts to extract information from QCD. In particular, some important results in the literature depend on an expansion in powers of $1/m_c$. We question whether this expansion is sufficiently understood and under control at present. Our model provides an explicit example of how far from the heavy quark limit the charm mass could, in fact, be. We will later discuss an example of a quantity receiving large $1/m_c$ corrections, and which also contributes to a measured branching ratio.

One of the prime applications of the heavy quark expansion is in the extraction of $|V_{cb}|$ from the processes $\bar{B} \rightarrow D^{(*)}\ell\bar{\nu}$ and $\Lambda_b \rightarrow \Lambda_c\ell\bar{\nu}$. In the heavy-quark limit $m_{b,c} \rightarrow \infty$, these processes are normalized in a model-independent way at zero hadronic recoil. But for any realistic m_c in our model there are always large positive deviations in at least one of $\bar{B} \rightarrow D^*\ell\bar{\nu}$ or $\bar{B} \rightarrow D\ell\bar{\nu}$ [2], concurrently with rather small deviations in $\Lambda_b \rightarrow \Lambda_c\ell\bar{\nu}$ [5]. The large deviations are a sensitive function of the quark masses, and their origin lies in the hyperfine interaction which splits the ground-state pseudoscalar and vector D mesons. This would lead to a discrepancy between the values of $|V_{cb}|$ extracted from these various processes under the assumption that the deviations from the heavy-quark limit are negligible.

In Fig. 1 we show that our model's prediction for the *shape* of the decay spectrum of $\bar{B} \rightarrow D^*\ell\bar{\nu}$ agrees well with the most recent CLEO data [9]. If we ignored our correction to the overall normalization and forced the heavy-quark limit normalization at zero recoil we would obtain $|V_{cb}| = 0.036$. Our correction to the normalization implies that the actual $|V_{cb}|$ could be 10% or 15% smaller.

This paper is divided into three parts. In Parts I and II we describe two major extensions of the model. In Part I we incorporate chiral and gauge symmetries to deal with various processes involving pions and photons. In particular the ratio $\Gamma(D^{*0} \rightarrow D^0\pi^0)/\Gamma(D^{*0} \rightarrow D^0\gamma)$ is well measured experimentally and provides a sensitive probe to the physics of the light degrees of freedom in the D mesons. This will help constrain the only parameters

appearing in our model, the quark masses. Our model reproduces this branching ratio for a choice of quark masses very close to what we have previously used, and in particular it constrains our model m_c to be close to 1.45 GeV. We have observed before that $m_b - m_c$ was much more constrained by our model than $m_b + m_c$; the constraint reads $m_b - m_c = 3.36 \pm 0.03$ GeV (see the wedge-shaped region in Fig. 6 of [3]). With our new constraint on m_c , our model m_b must be close to our previously-used value of 4.8 GeV.

One ingredient in our calculation of $\Gamma(D^{*0} \rightarrow D^0\pi^0)/\Gamma(D^{*0} \rightarrow D^0\gamma)$ is the heavy-quark contribution to the $D^*D\gamma$ coupling. We find large $1/m_c$ corrections to this quantity, which are analogous to the large corrections we find in semileptonic B decays. For the $D^*D\pi$ and $D^*D\gamma$ couplings we find values which are one-third as large as the nonrelativistic quark model predictions. The small $D^*D\pi$ coupling has implications for calculations in heavy-quark chiral perturbation theory, and in particular the quantity $\Delta_D \equiv (M_{D_s^*} - M_{D_s}) - (M_{D^*} - M_D)$. We also include a discussion of charge radii.

We then consider the nonresonant contributions to the processes $\bar{B}^0 \rightarrow D^{(*)}\pi\ell\bar{\nu}$ in the context of the problem of the missing exclusive semileptonic \bar{B}^0 decay modes. The branching fraction for $\bar{B}^0 \rightarrow \ell\bar{\nu} + \text{anything}$ is $(9.5 \pm 1.6)\%$, while those for the dominant exclusive modes $\bar{B}^0 \rightarrow D^+\ell\bar{\nu}$ and $\bar{B}^0 \rightarrow D^*(2010)^+\ell\bar{\nu}$ are $(1.9 \pm 0.5)\%$ and $(4.4 \pm 0.4)\%$, respectively [10]. The model indicates that the nonresonant contributions play an important role in accounting for the discrepancy.

In Part II we extend the model to include seven excited charmed mesons. From the masses (or estimates of the masses) of these mesons we are able to determine appropriate model vertex functions. We calculate and display the various amplitudes for semileptonic B meson decays into these excited states. Our results for the various decay widths and electron energy spectra are in qualitative agreement with those of other authors. We confirm in particular that the decay rates to excited D 's are too small to account for the above mentioned discrepancy in semileptonic B decays.

In Part III we present some details of the heavy-quark limit of the model as it applies to the excited D 's. The full-model form factors deviate considerably from their values in the heavy-quark limit, as expected since the masses of these states are significantly greater than the charm-quark mass. We include the heavy-quark-limit results primarily for comparison with other models.

Also in Part III we study two modifications of the model. We first study the possible modification necessary to describe strange mesons, and in particular the process $B^+ \rightarrow \bar{K}^{*0}e^+\nu$. We address the question of whether the s should be treated as heavy or light. And second, we investigate the effect of modifying the form of the momentum damping at the basic quark-antiquark-meson vertex of the model. We consider an exponential damping factor, and we recover our previous conclusion that there is always a large positive deviation from the heavy-quark limit in one of $\bar{B} \rightarrow D^*\ell\bar{\nu}$ or $\bar{B} \rightarrow D\ell\bar{\nu}$.

Part I

Gauge and chiral symmetries

We begin with the light-quark triplet and triplets of pseudoscalar or vector meson fields H_Q with heavy quark Q .

$$\begin{array}{c} Q \\ b \\ c \end{array} H_Q \sim \begin{array}{c} (Q\bar{u}, Q\bar{d}, Q\bar{s}) \\ (B^-, \bar{B}^0, \bar{B}_s^0) \\ (D^0, D^+, D_s^+) \end{array} \quad \text{and} \quad q = \begin{pmatrix} u \\ d \\ s \end{pmatrix} \quad (1)$$

Under local $SU(3)_{V \times A}$ transformations with external vector and axial-vector fields V_μ and A_μ transforming as

$$V_\mu + A_\mu \gamma_5 \rightarrow G(V_\mu + A_\mu \gamma_5)G^\dagger + iG\partial_\mu G^\dagger, \quad (2)$$

the quark fields transform according to $Q \rightarrow Q$ and $q \rightarrow Gq$, where $G = \exp(i[\theta_V + \theta_A \gamma_5])$.

We define $\xi = \exp(i\mathcal{M}\gamma_5/f_\pi)$, where $f_\pi \simeq 132$ MeV and

$$\mathcal{M} = \begin{pmatrix} \frac{1}{\sqrt{2}}\pi^0 + \frac{1}{\sqrt{6}}\eta & \pi^+ & K^+ \\ \pi^- & -\frac{1}{\sqrt{2}}\pi^0 + \frac{1}{\sqrt{6}}\eta & K^0 \\ K^- & \bar{K}^0 & -\frac{2}{\sqrt{6}}\eta \end{pmatrix}. \quad (3)$$

Then ξ transforms as $\xi \rightarrow g\xi G^\dagger$.

The gauge-invariant version of the interaction Lagrangian is

$$\mathcal{L}_{\text{int}} = \sum_{Q=b,c} \sum_H \int dy \bar{Q}(x) \mathcal{L}_H(x, y) F_H(x-y) + \text{h.c.}, \quad (4)$$

where the function $F_H(x-y)$ is the Fourier transform of the damping factor,

$$F_H(x-y) = \int \frac{d^4k}{(2\pi)^4} e^{-ik \cdot (x-y)} \left(\frac{Z_H^2}{-k^2 + \hat{\Lambda}_H^2} \right)^n. \quad (5)$$

For the ground-state mesons, $n = 1$ and $\mathcal{L}_H(x, y)$ are given by

$$\begin{array}{c} H \\ 1 \ 0_{1/2}^- \\ 1 \ 1_{1/2}^- \end{array} \frac{\mathcal{L}_H(x, y)}{-iH_Q(x)\gamma_5 K(x, y)\xi(y)q(y)} \quad (6)$$

$$iH_Q(x)K(x, y)\xi(y)q(y).$$

The quantity $K(x, y)$ is a path-ordered exponential

$$K(x, y) = \text{P exp} \left\{ i \int_y^x dz^\mu \Gamma_\mu(z) \right\}, \quad (7)$$

where

$$\Gamma_\mu = \frac{1}{2}\xi[i\partial_\mu + V_\mu + A_\mu \gamma_5]\xi^\dagger + \frac{1}{2}\xi^\dagger[i\partial_\mu + V_\mu - A_\mu \gamma_5]\xi \quad (8)$$

Under the $SU(3)_{V \times A}$ transformations, $K(x, y) \rightarrow g(x)K(x, y)g^\dagger(y)$, and the meson fields transform as $H_Q \rightarrow H_Q g^\dagger$.

Mass terms involve an $SU(3)_{V \times A}$ -invariant piece and an $SU(3)_{V \times A}$ -breaking piece.

$$\mathcal{L}_{\text{mass}} = -\bar{q}(m\xi^2 + \mathcal{M}_q)q, \quad (9)$$

where we take $m \sim 250$ MeV and $\mathcal{M}_q = \text{diag}(m_u^{\text{curr}}, m_d^{\text{curr}}, m_s^{\text{curr}}) \sim (0, 0, 170)$ MeV. When $\mathcal{M}_q = 0$, the full Lagrangian

$$\mathcal{L} = \bar{Q}(i\cancel{\partial} - m_Q)Q + \bar{q}(i\cancel{\partial} + \cancel{V} + \cancel{A}\gamma_5)q + \mathcal{L}_{\text{mass}} + \mathcal{L}_{\text{int}} \quad (10)$$

is invariant under the local $SU(3)_{V \times A}$ transformations.

$D^* \rightarrow D\pi$ and $D^* \rightarrow D\gamma$

In this section we describe our calculation of $\Gamma(D^{*0} \rightarrow D^0\pi^0)/\Gamma(D^{*0} \rightarrow D^0\gamma)$. This quantity depends sensitively on the only two parameters appearing in our model for D mesons, the charm mass and the light quark mass m . We will show that a parameter choice which gives an acceptable result is $m_c = 1450$ MeV and $m = 270$ MeV. The main point is that these values are close to the values, $m_c = 1440$ MeV and $m = 250$ MeV, appearing in our previous work. For consistency with our previous results we will continue to use our old parameter choice in all other sections of this paper. Except where noted, our results in other sections do not display such a large sensitivity to quark masses.

In this section we shall also be comparing the D meson results to B meson and heavy-quark limit results. For the b quark mass we adopt our previous value, $m_b = 4.8$ GeV, as explained above.

We first consider the matrix element

$$f_\pi \langle H^0(M'v')\pi^+(l) | H^{*+}(Mv, \varepsilon) \rangle = \sqrt{MM'}(\omega + 1)h^{H\pi}(\omega)l \cdot \varepsilon. \quad (11)$$

We define $g_{H^*H\pi} \equiv h^{H\pi}(1)$. This can be calculated using the pion couplings derived above, or it can be extracted more simply by inserting the axial current on the light-quark line. Our results are $g_{D^*D\pi} = 0.28$ and $g_{B^*B\pi} = 0.32$. The first two terms in the heavy-quark expansion are

$$g_{H^*H\pi} = 0.34 - 0.17 \frac{\bar{\Lambda}}{m_Q}, \quad (12)$$

where $\bar{\Lambda} \equiv M - m_Q \simeq 500$ MeV is the lowest-order difference between the meson and heavy-quark masses. These numbers are in agreement with other relativistic models and sum rules [12][13][14], and they are in marked contrast to the nonrelativistic quark model which gives a value of unity.

We next consider the matrix element of the electromagnetic current, and we distinguish the light- and heavy-quark contributions.

$$\langle H_Q(M'v') | J_\mu^{\text{e.m.}} | H_Q^*(Mv, \varepsilon) \rangle = \sqrt{MM'} [e_q h_q^{H\gamma}(\omega) + e_Q h_Q^{H\gamma}(\omega)] i\varepsilon_{\mu\nu\rho\sigma} \varepsilon^\nu v'^\rho v^\sigma. \quad (13)$$

For the light-quark contribution we find $h_q^{D\gamma}(1) = 1.56$ and $h_q^{B\gamma}(1) = 5.00$. The first two terms in the heavy-quark expansion are

$$h_q^{H\gamma}(1) = 0.50 \frac{m_Q}{\bar{\Lambda}} \left(1 + 0.47 \frac{\bar{\Lambda}}{m_Q} \right). \quad (14)$$

The light-quark contribution is not predicted by heavy-quark symmetry, but the nonrelativistic quark model predicts a value for $h_q^{H\gamma}(1)$ of order the heavy-quark to light-quark mass ratio. Our result is about a factor of three smaller, which mirrors the situation with the pion coupling. In both cases, the relevant diagram involves either a vector or axial coupling to the light quark line. The suppression associated with the relativistic nature of the diagram seems to apply to both cases equally. We also note that in both cases the heavy-quark expansion provides a good representation of the full-model results.

The situation is different for the heavy-quark contribution to the $DD^*\gamma$ couplings. We find $h_Q^{D\gamma}(1) = 1.54$ and $h_Q^{B\gamma}(1) = 1.16$, to be compared with the first two terms in the heavy-quark expansion

$$h_Q^{H\gamma}(1) = 1 + \frac{\bar{\Lambda}}{m_Q} (1 - \xi_3(1)). \quad (15)$$

The latter gives $h_Q^{D\gamma}(1) = 1.35$ and $h_Q^{B\gamma}(1) = 1.10$. ($\xi_3(1)$ is negligible in our model [1].) The deviations from the heavy-quark expansion are much more significant here than they are for the pion and photon couplings to the light quark. As we have said, these large corrections are analogous to the large $1/m_c$ corrections we find for V_{cb} .

We now use the above results to extract the $D\pi$ and $D\gamma$ decay widths of the D^* . We find $\Gamma(D^{*+} \rightarrow D^0\pi^+) + \Gamma(D^{*+} \rightarrow D^+\pi^0) = 20.9$ KeV and $\Gamma(D^{*0} \rightarrow D^0\pi^0) = 9.4$ KeV. For the radiative decay branching fractions we also display the effect of the leading SU(3) breaking corrections calculated in [11]. We obtain

	experiment	with corrections	without corrections	
B($D^{*0} \rightarrow D^0\gamma$) (%)	36.4 ± 2.8	37.8	45.6	(16)
B($D^{*+} \rightarrow D^+\gamma$) (%)	$1.1 \begin{smallmatrix} +1.4 \\ -0.7 \end{smallmatrix}$	2.9	2.1	

The agreement in the first two columns is a reflection of the quark masses we have chosen.

We consider briefly the implications for the SU(3)-violating quantities $\Delta_H \equiv (M_{H_s^*} - M_{H_s}) - (M_{H^*} - M_H)$. It was stressed in [15] that the measured values, $\Delta_D = 0.9 \pm 1.9$ MeV and $\Delta_B = 1.2 \pm 2.7$ MeV, are much smaller than expected from the leading SU(3)-breaking one-loop contribution. It was estimated that this source alone gives $\Delta_D^{\text{one loop}} \approx -47$ MeV and $\Delta_B^{\text{one loop}} \approx -16$ assuming that $g_{D^*D\pi}^2 = 0.5$. Using our values of $g_{D^*D\pi}$ and $g_{B^*B\pi}$ instead would yield the less problematic numbers $\Delta_D^{\text{one loop}} \approx -7$ MeV and $\Delta_B^{\text{one loop}} \approx -3$.

Charge radii

Gauge-invariance of the Lagrangian (10) implies extra Feynman rules for the matrix elements of the light-quark vector current between two mesons. The photon can attach to the nonlocal

vertices as well as to the quark lines. The new Feynman rule for a vertex with outgoing photon momentum q and outgoing light-quark momentum k is

$$\frac{-i(2k+q)_\mu \gamma_5 (\not{\epsilon}^*) Z^2}{[-k^2 + \hat{\Lambda}^2][-(k+q)^2 + \hat{\Lambda}^2]}. \quad (17)$$

This must be included in the computation of the light-quark contribution to the electromagnetic charge radius of the meson (although it did not appear in the above calculation of the $DD^*\gamma$ coupling).

Define the matrix element of the electromagnetic current by

$$\langle H_Q(p') | J_\mu^{\text{e.m.}} | H_Q(p) \rangle = [-e_q F_q(q^2) + e_Q F_Q(q^2)](p+p')_\mu, \quad (18)$$

where $e_c = e_u = 2/3$ and $e_b = e_d = -1/3$ and we have decomposed the form factor into light-quark and heavy-quark contributions with $F_q(0) = 1 = F_Q(0)$. We define $r_i = [6\partial F_i/\partial q^2(0)]^{1/2}$ for $i = q, Q$. As an example we compare the contributions to the charge radius of the ground state pseudoscalar ($L = 0$) D to one of the excited states treated in Part II, the scalar ($L = 1$) D_0^* .

H	$1/r_q(\text{MeV})$	$1/r_Q(\text{MeV})$	
D	300	830	(19)
D_0^*	690	830	

The 300 MeV vs. 690 MeV shows that the excited state is more compact than the ground state, as might be expected due to the higher energy present in the light-quark system in the excited state. This effect is not present in models of nonrelativistic quarks.

We also note that the large light-quark charge radius of the D reflects a rapid damping of the form factor in q^2 when the current attaches to the light-quark line. We will use this fact when discussing nonresonant contributions to semileptonic decays in which a pion attaches to the light-quark line.

Nonresonant processes

The data indicate that the decays $\bar{B}^0 \rightarrow D^+ \ell \bar{\nu}$ and $\bar{B}^0 \rightarrow D^*(2010)^+ \ell \bar{\nu}$ contribute only 66% of the total semileptonic width $\bar{B}^0 \rightarrow \ell \bar{\nu} + \text{anything}$. We will find in Part II that resonant decays to the eight lowest lying excited D 's account for a further 6%. This leaves 28% missing. It is safe to assume that this will not be made up by decays into even higher lying D excitations. And neither will it be decays to final states other than charm, in view of the smallness of $|V_{ub}|$. The implication is that a significant portion of the total width must be into nonresonant charmed final states. The nonresonant width must be of order $1.6 \times 10^{13} |V_{cb}|^2 \text{ s}^{-1}$.

We consider nonresonant contributions to the processes $\bar{B}^0 \rightarrow D^{(*)} \pi \ell \bar{\nu}$ in our model. The Lagrangian (10) gives rise to three graphs, one with a pion coming off the light-quark line (proportional to the common mass m) and two with pions coming off the vertices. The sum of these three graphs is the same as an insertion of $f_\pi^{-1} l_\mu \gamma^\mu \gamma_5$ on the light-quark line, where

l is the pion momentum. Because of the difficulties involved in computing the resulting four-point graph, we were able only to obtain the hadronic matrix element in the soft-pion limit, i.e. keeping only terms linear in l . In this limit, we define form factors $q_i(\omega)$ and $r_i(\omega)$ (with $\omega = v \cdot v'$ as usual) by

$$f_\pi \langle D^0(M_D v') \pi^+(l) | \bar{c} \gamma_\mu (1 - \gamma_5) b | \bar{B}^0(M_B v) \rangle = q_V i \varepsilon_{\mu\nu\rho\sigma} v^\nu l^\rho v'^\sigma - q_{A_1} l_\mu - [q_{A_2} l \cdot v + q_{A_3} l \cdot v'] v_\mu - [q_{A_4} l \cdot v + q_{A_5} l \cdot v'] v'_\mu. \quad (20)$$

and

$$f_\pi \langle D^{*0}(M_{D^*} v') \pi^+(l) | \bar{c} \gamma_\mu (1 - \gamma_5) b | \bar{B}^0(M_B v) \rangle = \varepsilon \cdot v [r_{V_1} l_\mu + (r_{V_2} v \cdot l + r_{V_3} v' \cdot l) v_\mu + (r_{V_4} v \cdot l + r_{V_5} v' \cdot l) v'_\mu] + (r_{V_6} v \cdot l + r_{V_7} v' \cdot l) \varepsilon_\mu + (r_{V_8} v_\mu + r_{V_9} v'_\mu) l \cdot \varepsilon - i \varepsilon_{\mu\nu\rho\sigma} \varepsilon^\nu [r_{A_1} v'^\rho v^\sigma + l^\rho (r_{A_2} v^\sigma + r_{A_3} v'^\sigma)]. \quad (21)$$

The values of the above form factors at $\omega = 1$ are

$$\frac{q_V \quad q_{A_1} \quad q_{A_2} \quad q_{A_3} \quad q_{A_4} \quad q_{A_5}}{14.8 \quad 24.0 \quad -3.5 \quad -8.2 \quad -4.6 \quad -2.7} \quad (22)$$

and

$$\frac{r_{V_1} \quad r_{V_2} + r_{V_3} + r_{V_4} + r_{V_5} \quad r_{V_6} + r_{V_7} \quad r_{V_8} + r_{V_9} \quad r_{A_2} + r_{A_3}}{-1.7 \quad 11 \quad -0.1 \quad -20.1 \quad 19.5} \quad (23)$$

The rather large magnitude of some of these dimensionless hadronic quantities is striking. The amplitude vanishes for vanishing pion momenta, and it rapidly increases for increasing pion momentum up to some momenta of order 300 or 400 MeV (roughly the inverse of the charge radius), after which the amplitude will decrease. We choose a small value of the pion momentum (equal to the pion mass) well below where the amplitude peaks. We set $v = v'$, let the massless electron and antineutrino emerge with equal energies, and then perform the four-body phase space integral with this constant matrix element squared. The result is $\Gamma(\bar{B}^0 \rightarrow D^0 \pi^+ \ell \bar{\nu}) \sim 0.6 \times 10^{13} |V_{cb}|^2 \text{ s}^{-1}$ and $\Gamma(\bar{B}^0 \rightarrow D^{*0} \pi^+ \ell \bar{\nu}) \sim 0.3 \times 10^{13} |V_{cb}|^2 \text{ s}^{-1}$.¹ The decays with charged D and neutral pion are half as large. The total nonresonant width is then $\sim 1.8 \times 10^{13} |V_{cb}|^2 \text{ s}^{-1}$, in rough agreement with the value deduced above. While this crude estimate is far from being a definite prediction, it does make reasonable the possibility that nonresonant decays make an important contribution to the semileptonic width of the B meson.

Part II

Description of model for excited mesons

Our notation is $N J_{j_\ell}^P$, where N labels the radial excitation, J^P is the meson spin-parity, and j_ℓ is the total angular momentum of the light degrees of freedom. It is the sum of orbital

¹These results are also quite sensitive to the quark masses used. For example, if our “new” values of the masses are used then $\Gamma(\bar{B}^0 \rightarrow D^0 \pi^+ \ell \bar{\nu})$ increases by 40%.

angular momentum L and light-quark spin $s_\ell = 1/2$. This paper will treat the eight $N = 1$ states shown in (24), where the masses in the last column corresponding to question marks are estimates. The naming convention is that of the Particle Data Group [10].

N	L	j_ℓ	doublet	name	mass
1	1	1/2	$\begin{pmatrix} 1 \ 0_{1/2}^- \\ 1 \ 1_{1/2}^- \end{pmatrix}$	D	1869
				$D^*(2010)$	2010
1	1	1/2	$\begin{pmatrix} 1 \ 0_{1/2}^+ \\ 1 \ 1_{1/2}^+ \end{pmatrix}$	$D_0^*(?)$	2465
				$D_1^*(?)$	2270
1	1	3/2	$\begin{pmatrix} 1 \ 1_{3/2}^+ \\ 1 \ 2_{3/2}^+ \end{pmatrix}$	$D_1(2420)$	2421
				$D_2^*(2460)$	2465
1	2	3/2	$\begin{pmatrix} 1 \ 1_{3/2}^- \\ 1 \ 2_{3/2}^- \end{pmatrix}$	$D^*(?)$	2800
				$D_2^*(?)$	2800

In addition, we will consider the first radial excitation $2 \ 0_{1/2}^-$ with an estimated mass of 2440 MeV. As is commonly done [17], we will ignore possible mixing between $1 \ 1_{1/2}^+$ and $1 \ 1_{3/2}^+$.

The interaction vertices between hadron, heavy quark, and light degrees of freedom are chosen in the following way. Each vertex is the product of some gamma-matrix structure and a damping factor. The gamma-matrix structure is chosen to be identically equal to the form determined by heavy-quark symmetry [18]. This is required for consistency with QCD in the heavy-quark limit. The damping factor is chosen to be a sum of terms of the form $[Z^2/(-k^2 + \hat{\Lambda}^2)]^n$, where the least power n is chosen to be the smallest which guarantees the convergence of the relevant integrals, and where Z and $\hat{\Lambda}$ are different for each state. We use standard quark propagators throughout.

We take the interaction Lagrangian to be that given in (4) where $\mathcal{L}_H(x, y)$ and the powers n are given by

H	$\mathcal{L}_H(x, y)$	n
$1 \ 0_{1/2}^-$	$-iH(x)\gamma_5 q(y)$	1
$1 \ 1_{1/2}^-$	$i\mathbb{H}(x)q(y)$	1
$1 \ 0_{1/2}^+$	$iH(x)q(y)$	1
$1 \ 1_{1/2}^+$	$i\mathbb{H}(x)\gamma_5 q(y)$	1
$1 \ 1_{3/2}^+$	$\frac{1}{\Lambda}\sqrt{\frac{3}{2}}H_\mu(x)\gamma_5\left\{g^{\mu\nu} - \frac{1}{3}\gamma^\mu(\gamma^\nu - v^\nu)\right\}\partial_\nu q(y)$	2
$1 \ 2_{3/2}^+$	$\frac{1}{\Lambda}H^{\mu\nu}(x)\gamma_\mu\partial_\nu q(y)$	2
$1 \ 1_{3/2}^-$	$\frac{1}{\Lambda}\sqrt{\frac{3}{2}}H_\mu(x)\left\{g^{\mu\nu} - \frac{1}{3}\gamma^\mu(\gamma^\nu + v^\nu)\right\}\partial_\nu q(y)$	2
$1 \ 2_{3/2}^-$	$\frac{1}{\Lambda}H^{\mu\nu}(x)\gamma_\mu\gamma_5\partial_\nu q(y)$	2
$2 \ 0_{1/2}^-$	$-iH(x)\gamma_5 q(y)$	$1 + 2$.

Wherever a velocity v occurs in (25), it is the velocity of the external meson (and not that of the heavy quark).

The only parameters of the model are the quark masses; the various Z 's and $\hat{\Lambda}$'s are fixed via the meson ‘‘mass functions’’ $\Sigma(p^2)$. These are defined in terms of the meson self-energy graphs, which are given by $i\Sigma(p^2)$, $-ig_{\mu\nu}\Sigma(p^2) + \dots$ and $ig_{\mu\nu}g_{\rho\sigma}\Sigma(p^2) + \dots$ when $J = 0, 1$ and 2, respectively. First $\hat{\Lambda}$ is fixed by setting $\Sigma(M^2) = 0$. Then, Z is fixed by setting

$\Sigma'(M^2) = 1$, where prime denotes differentiation with respect to p^2 . This latter condition is equivalent to conservation of the heavy-quark vector current by the Ward identity.

The situation is a little more complicated in the case of the radial excitation $2\ 0_{1/2}^-$ of the ground-state pseudoscalar $1\ 0_{1/2}^-$. We take the damping factor to be a linear combination of $n = 1$ and $n = 2$, which we write as

$$\frac{Z^2}{-k^2 + \hat{\Lambda}^2} \left[1 + f \frac{\hat{\Lambda}^2}{-k^2 + \hat{\Lambda}^2} \right]. \quad (26)$$

First, f and Z are determined as functions of $\hat{\Lambda}$ at fixed quark and meson masses by the zero and the slope of the mass function. Then, $\hat{\Lambda}$ is determined by the vanishing of the matrix element $\langle 1\ 0_{1/2}^- | \bar{Q} \gamma_\mu Q | 2\ 0_{1/2}^- \rangle$ at $q^2 = 0$, as required by current conservation.

The values of the various constants are given in (27) in MeV. Quark masses $m_c = 1440$ and $m_q = 250$ MeV have been used.

H	$\hat{\Lambda}_H$	Z_H	
$1\ 0_{1/2}^-$	537	745	
$1\ 1_{1/2}^-$	762	1193	
$1\ 0_{1/2}^+$	1217	1838	
$1\ 1_{1/2}^+$	1065	1881	
$1\ 1_{3/2}^+$	1400	2143	(27)
$1\ 2_{3/2}^+$	1359	2122	
$1\ 1_{3/2}^-$	1976	3231	
$1\ 2_{3/2}^-$	1745	2804	
$2\ 0_{1/2}^-$	1430	2594	

We find $f = -1.1$ for the $2\ 0_{1/2}^-$ state. In addition, we need the values appropriate to the B and B^* : $m_b = 4800$, $\hat{\Lambda}_B = 621$, $\hat{\Lambda}_{B^*} = 702$, $Z_B = 1103$, and $Z_{B^*} = 1290$ MeV.

The resonant processes $\bar{B} \rightarrow H \ell \bar{\nu}$

We now consider the hadronic matrix elements

$$\mathcal{M}_\mu^H = \frac{1}{\sqrt{MM'}} \langle H(M'v') | \bar{c} \gamma_\mu (1 - \gamma_5) b | \bar{B}(Mv) \rangle, \quad (28)$$

where H denotes any of the D states. The matrix elements may be written as

H	\mathcal{M}_μ^H	
$1\ 0_{1/2}^-$	$S(a_+, a_-)_\mu$	
$1\ 1_{1/2}^-$	$T(b_V, b_{A_1}, b_{A_2}, b_{A_3})_{\mu\nu}\varepsilon^{*\nu}$	
$1\ 0_{1/2}^+$	$-S(c_+, c_-)_\mu$	
$1\ 1_{1/2}^+$	$-T(d_A, d_{V_1}, d_{V_2}, d_{V_3})_{\mu\nu}\varepsilon^{*\nu}$	
$1\ 1_{3/2}^+$	$-T(f_A, f_{V_1}, f_{V_2}, f_{V_3})_{\mu\nu}\varepsilon^{*\nu}$	
$1\ 2_{3/2}^+$	$T(g_V, g_{A_1}, g_{A_2}, g_{A_3})_{\mu\nu}\varepsilon^{*\nu\lambda}v_\lambda$	
$1\ 1_{3/2}^-$	$T(h_V, h_{A_1}, h_{A_2}, h_{A_3})_{\mu\nu}\varepsilon^{*\nu}$	
$1\ 2_{3/2}^-$	$-T(k_A, k_{V_1}, k_{V_2}, k_{V_3})_{\mu\nu}\varepsilon^{*\nu\lambda}v_\lambda$	
$2\ 0_{1/2}^-$	$S(l_+, l_-)_\mu$	

(29)

where

$$\begin{aligned}
S(a_+, a_-)_\mu &= a_+(v + v')_\mu + a_-(v - v')_\mu \\
T(b_V, b_{A_1}, b_{A_2}, b_{A_3})_{\mu\nu} &= ib_V\varepsilon_{\mu\nu\rho\sigma}v'^\rho v^\sigma - b_{A_1}g_{\mu\nu} - (b_{A_2}v_\mu + b_{A_3}v'_\mu)v_\nu.
\end{aligned}
\tag{30}$$

We take the form factors to be functions of $\omega = v \cdot v'$; e.g. $a_+ \equiv a_+(\omega)$.

The form factors a_\pm and b_i of (29) and (30) become proportional to the ‘‘original’’ Isgur-Wise function $\xi \equiv \xi_{1/2}$ in the heavy-quark limit $m_{b,c} \rightarrow \infty$. Similarly, c_\pm and d_i become proportional to $\tau_{1/2}$, f_i and g_i to $\tau_{3/2}$, and h_i and k_i to $\xi_{3/2}$. The form factors l_\pm for decay into the radially-excited state become proportional to $\xi_{1/2}^{(2)}$. The coefficients of proportionality are shown in (31).

units	form factors in given units	
$\xi_{1/2}$	$a_+ = 1$	$a_- = 0$
	$b_V = 1$	$b_{A_1} = \omega + 1$
	$b_{A_2} = 0$	$b_{A_3} = -1$
$\tau_{1/2}$	$c_+ = 0$	$c_- = -2$
	$d_{V_1} = 2(\omega - 1)$	$d_{V_2} = 0$
	$d_{V_3} = -2$	$d_A = 2$
$\tau_{3/2}$	$f_{V_1} = -\frac{\omega^2-1}{\sqrt{2}}$	$f_{V_2} = -\frac{3}{\sqrt{2}}$
	$f_{V_2} - f_{V_3} = -\frac{\omega+1}{\sqrt{2}}$	$f_A = -\frac{\omega+1}{\sqrt{2}}$
	$g_V = \sqrt{3}$	$g_{A_1} = \sqrt{3}(\omega + 1)$
	$g_{A_2} = 0$	$g_{A_3} = -\sqrt{3}$
$\xi_{3/2}$	$h_V = \frac{\omega-1}{\sqrt{2}}$	$h_{A_1} = \frac{\omega^2-1}{\sqrt{2}}$
	$h_{A_2} = \frac{3}{\sqrt{2}}$	$h_{A_2} + h_{A_3} = -\frac{\omega-1}{\sqrt{2}}$
	$k_{V_1} = \sqrt{3}(\omega - 1)$	$k_{V_2} = 0$
	$k_{V_3} = -\sqrt{3}$	$k_A = \sqrt{3}$
$\xi_{1/2}^{(2)}$	$l_+ = \omega - 1$	$l_- = 0$

(31)

Our results for the various full-model form factors for B decays into the excited D states are represented in Figs. 2-4. In order to facilitate comparison with the heavy-quark limit, we have chosen not to plot the full-model form factors directly, but rather to divide out the coefficients in (31). This puts all form factors on a comparable scale, and shows the ‘‘effective’’

Isgur-Wise functions which would be extracted from the data under the assumption that the deviations from the heavy-quark limit were small. In those cases where the coefficient vanishes at $\omega = 1$, we have subtracted off the zero-recoil value before dividing by the coefficient. For example, the curve labelled “ d_{V_1} ” in Fig. 2 is equal to $[d_{V_1}(\omega) - d_{V_1}(1)]/2(\omega - 1)$. In those cases where the coefficient vanishes identically, we have omitted the corresponding full-model form factor for brevity.

Fig. 5 shows a comparison between the full-model form factors for B decays into the ground state pseudoscalar D and its first radial excitation. We note the strong suppression of the form factors for the latter.

The various decay widths are given by

$$\Gamma_H = |V_{cb}|^2 \frac{G_F^2 M^5 r^3}{48\pi^3} \int_1^{(1+r^2)/2r} d\omega \sqrt{\omega^2 - 1} \mathcal{F}_H(\omega), \quad (32)$$

where $r = M'/M$. The functions \mathcal{F}_H are given by

H	$\mathcal{F}_H(\omega)$	
$1\ 0_{1/2}^-$	$F_0(a_+, a_-)$	
$1\ 1_{1/2}^-$	$2F_T(b_V, b_{A_1}) + F_L(b_{A_1}, b_{A_2}, b_{A_3})$	
$1\ 0_{1/2}^+$	$F_0(c_+, c_-)$	
$1\ 1_{1/2}^+$	$2F_T(d_A, d_{V_1}) + F_L(d_{V_1}, d_{V_2}, d_{V_3})$	
$1\ 1_{3/2}^+$	$2F_T(f_A, f_{V_1}) + F_L(f_{V_1}, f_{V_2}, f_{V_3})$	(33)
$1\ 2_{3/2}^+$	$(\omega^2 - 1)\{F_T(g_V, g_{A_1}) + \frac{2}{3}F_L(g_{A_1}, g_{A_2}, g_{A_3})\}$	
$1\ 1_{3/2}^-$	$2F_T(h_V, h_{A_1}) + F_L(h_{A_1}, h_{A_2}, h_{A_3})$	
$1\ 2_{3/2}^-$	$(\omega^2 - 1)\{F_T(k_A, k_{V_1}) + \frac{2}{3}F_L(k_{V_1}, k_{V_2}, k_{V_3})\}$	
$2\ 0_{1/2}^-$	$F_0(l_+, l_-)$,	

where

$$\begin{aligned} F_0(a_+, a_-) &= (\omega^2 - 1)[(1+r)a_+ - (1-r)a_-]^2 \\ F_T(b_V, b_{A_1}) &= (1 - 2r\omega + r^2)[(\omega^2 - 1)b_V^2 + b_{A_1}^2] \\ F_L(b_{A_1}, b_{A_2}, b_{A_3}) &= [(\omega - r)b_{A_1} + (\omega^2 - 1)(rb_{A_2} + b_{A_3})]^2. \end{aligned} \quad (34)$$

We compare our model results for the full rates Γ_H with those of other models in (35), in units of $10^{13}|V_{cb}|^2\text{ s}^{-1}$. (Note that $1_{1/2}^+$ and $1_{3/2}^+$ are linear combinations of 1P_1 and 3P_1 . Results computed in the latter basis are denoted by asterisks in (35), and “HQ” denotes heavy-quark limit results.)

N	$J_{j\ell}^P$	ISGW	CNP	ours	ours	CNP	Suzuki
		(full) [19]	(full) [20]	(full)	(HQ)	(HQ) [21]	(HQ) [22]
1	$0_{1/2}^-$	1.25	0.76	0.900	0.771	0.723	0.741
1	$1_{1/2}^-$	3.24	2.3	2.91	2.32	2.22	2.20
1	$0_{1/2}^+$	0.049	0.076	0.028	0.013	0.026	0.011
1	$1_{1/2}^+$	0.180*		0.040	0.026	0.036	0.015
1	$1_{3/2}^+$	0.045*	0.076*	0.117	0.070	0.052	0.034
1	$2_{3/2}^+$	0.061		0.076	0.104	0.103	0.049
1	$1_{3/2}^-$			0.0021	0.0002		0.0007
1	$2_{3/2}^-$			0.0003	0.0002		0.0007
2	$0_{1/2}^-$	0.013		0.055			0.045
2	$1_{1/2}^-$	0.010					0.115

(35)

There are clear similarities among the various models. At the same time, measurements of these exclusive resonant processes could potentially discriminate between the models.

In Fig. 6 we show the electron energy spectra for the various resonant final D states and their total contribution to the inclusive B decay spectrum. The location of the maximum agrees with ISGW [19]. Fig. 7 shows the spectra of the excited D final states in more detail.

Part III

Some details of the heavy-quark limit.

We first recover one of the basic properties of heavy quark effective theory. The following is satisfied identically:

$$\langle P | \bar{Q}(x)(i\cancel{\partial} - m_Q)Q(x) | P \rangle = 0 \quad (36)$$

when the pseudoscalar meson P is on shell. This is easily seen because $i\cancel{\partial} - m_Q$ just removes one of the heavy-quark propagators from the graph for (36), leaving the P mass function evaluated at $p^2 = M^2$. This vanishes, by the definition of the mass. In the heavy-quark effective theory at lowest order we have $Q(x) \simeq \exp(-im_Q v \cdot x) h_v(x)$. Using $\cancel{\psi} h_v = h_v$, we find

$$\langle P | \bar{Q}(x)(i\cancel{\partial} - m_Q)Q(x) | P \rangle \simeq \langle P | \bar{h}_v(x) i\cancel{\partial} \cdot v h_v(x) | P \rangle = 0. \quad (37)$$

Thus we recover the equation of motion $iv \cdot Dh_v = 0$ of heavy quark effective theory; here $D = \partial$ since there are no gluons in the model.

The heavy-quark limit results in (35) are included for comparison purposes only. They have limited physical meaning since they are computed using the above formulae with Isgur-Wise functions for the form factors, while the meson masses are kept at their physical values.

It has become standard to display the differential ω spectrum by taking the square root of (32) and dividing out model-independent factors in such a way as to make the result equal to the corresponding Isgur-Wise function if the form factors are replaced by their values in the heavy-quark limit. This procedure is applied to the $1/2^+$ and $3/2^+$ final states (the

curves labelled “full”) in Figs. 8 and 9, respectively. We note the considerable deviations from the heavy-quark limit.

An important quantity is the lowest-order mass difference $\bar{\Lambda}$ between meson and heavy quark:

$$M = m_Q + \bar{\Lambda} + \mathcal{O}(\bar{\Lambda}^2/m_Q). \quad (38)$$

We extract the following approximate values for the $N = 1$ states:

$$\frac{j_\ell^P}{\bar{\Lambda}} \quad \begin{array}{cccc} 1/2^- & 1/2^+ & 3/2^+ & 3/2^- \end{array} \quad (39)$$

$$\frac{}{\bar{\Lambda}} \quad \begin{array}{cccc} 500 & 860 & 990 & 1330 \end{array}$$

These numbers make clear the breakdown of an expansion in $\bar{\Lambda}/m_c$ for the higher-lying states.

We also display the following zero-recoil values of the Isgur-Wise functions, along with our previous result [3] for the slope of the usual Isgur-Wise function $\xi \equiv \xi_{1/2}$ at zero recoil.

$$\frac{-\xi'_{1/2}(1) \quad \tau_{1/2}(1) \quad \tau_{3/2}(1) \quad \xi_{3/2}(1)}{1.28 \quad 0.21 \quad 0.29 \quad 0.013} \quad (40)$$

In comparison, the ISGW model result is $\tau_{1/2}(1) = \tau_{3/2}(1) = 0.315$ [23]. The QCD sum rule approach of [21] found $\tau_{1/2}(1) \simeq \tau_{3/2}(1) = 0.2$ to 0.25 ,² while the Bethe-Salpeter approach of [24] found $\tau_{1/2}(1) = 0.21$ and $\tau_{3/2}(1) = 0.44$.

Another issue is the extent to which the Bjorken sum rule is saturated by the states we have calculated. This sum rule reads [23]

$$-\xi'_{1/2}(1) = 1/4 + |\tau_{1/2}(1)|^2 + 2|\tau_{3/2}(1)|^2 + \dots \quad (41)$$

where the ellipsis denotes contributions from higher radial excitations, from states with quantum numbers other than $1/2^-$, $1/2^+$ and $3/2^+$, and from inelastic continua. We find numerically $1.28 = 0.25 + 0.04 + 0.17 + \dots = 0.46 + \dots$ for Eq. (41). The sum rule is far from being saturated by the resonances we have considered so far; this result reflects the situation already observed in the full model. As already stated, our model indicates that this is due mainly to nonresonant contributions to final states containing a pion. The discrepancy is even larger here because the sum rule was derived in the heavy-quark limit, and the D mesons are rather far from this limit in our model.

One last issue of current interest is the dependence of the slope of the Isgur-Wise function on the light-quark mass. We find that the slope increases when the light-quark mass is replaced by the strange-quark mass, from -1.28 to -1.55 . This behavior agrees with other analyses in quark models [25], sum rules [26] and lattice [27], but it disagrees with heavy-quark chiral perturbation theory [28]. Our dependence of the slope on the light-quark mass is given in [5], and it is far from linear.

The decay $D \rightarrow K^* \ell \nu$

We now explore how the model may be extended to describe strange mesons. We will consider the K^* and will avoid the K and its complicating pseudo-Goldstone nature. The

²The range of values reflects the conflict between Fig. 1 and Table 1 of [21].

process $D^+ \rightarrow \overline{K}^*(892)^0 e^+ \nu_e$ is of interest since models tend to disagree with the data by predicting a branching fraction which is larger than the measured value. For us, one option is to model the K^* exactly like we model the D^* and B^* mesons. This would be making the rather suspect assumption that the s quark acts like a heavy quark. The other option, perhaps equally suspect, is to treat the s quark as light, on the same footing as the u and d quarks. This would entail modifying the vertex damping factor in (5) in order to treat the \overline{d} and s symmetrically. The damping factor then becomes

$$\frac{Z^2}{-k_{\overline{d}}^2 + \widehat{\Lambda}^2} + \frac{Z^2}{-k_s^2 + \widehat{\Lambda}^2}. \quad (42)$$

We will give the results for these two options.

With a strange quark mass of $250 + 170 = 420$ MeV, we find $\widehat{\Lambda}_{K^*} = 598$ MeV and $Z_{K^*} = 836$ MeV. The relevant observables can be compared to the measured values as follows.[10]

	Γ_L/Γ_T	Γ_+/Γ_-	$B(D^+ \rightarrow \overline{K}^{*0} e^+ \nu_e)\%$
experiment	1.23 ± 0.13	0.16 ± 0.04	4.8 ± 0.4
model (heavy s)	0.99	0.24	8.1
model (light s)	1.04	0.25	2.8

(43)

We see that only the branching fraction is very sensitive to how the s quark is treated, and interestingly enough, the experimental branching fraction lies between the two extreme ways of treating the s .

We may also extract the form factors $V(q^2)$, $A_1(q^2)$ and $A_2(q^2)$ for $q^2=0$, which may then be compared to nonrelativistic quark model and to sum rule results. For additional models see [10].

	$V(0)$	$A_1(0)$	$A_2(0)$
model (heavy s)	1.14	0.76	0.82
model (light s)	0.68	0.48	0.52
ISGW	1.1	0.8	0.8
BBD	1.1	0.5	0.6
experiment	1.1 ± 0.2	0.56 ± 0.04	0.40 ± 0.08

(44)

Note that the experimental values here [10] have been extracted by assuming specific pole expressions for the form factors. We may compare those form factors to our model form factors by fitting our form factors in the physical region to the pole form $F(q^2) = F(0)/(1 - q^2/m_F^2)$. The values for m_F in GeV are the following.

	V	A_1	A_2
assumed in [10]	2.1	2.5	2.5
model (heavy s)	1.65	2.3	1.8
model (light s)	2.0	3.8	2.4

(45)

The form of the vertex damping factor

The model relies on a vertex damping factor to suppress the flow of large Euclidean momenta through light-quark propagators, and a specific pole form has been chosen.

$$F(k^2) = \frac{Z^2}{-k^2 + \widehat{\Lambda}^2} \quad (46)$$

This introduces singularities into our quark loop amplitudes for momenta outside the physical region [8]. Viewing our amplitudes as functions of the quark masses while keeping the meson masses fixed, there are also cusp-like singularities for special (presumably unphysical) values of the quark masses [3]. We wish to explore here how our conclusions depend on our choice of the damping factor, and on the singularity structure of the model in particular. To do this we will substitute an exponential form for the damping factor,

$$F(k^2) = R \exp\left(\frac{k^2}{\Delta^2}\right). \quad (47)$$

This may be less realistic for large $-k^2$, but it is free from unphysical singularities at finite $-k^2$. The parameters R and Δ will be determined for each meson from the self-energy graphs, as was done for the quantities Z and $\widehat{\Lambda}$ of (46). Our standard quark masses imply $R_B=3.81$, $\Delta_B=620$ MeV, $R_D=2.37$, $\Delta_D=518$ MeV, $R_{D^*}=2.96$ and $\Delta_{D^*}=785$ MeV. The shape of the exponential damping factor is compared to the original damping factor for the B meson in Fig. 10.

We give the values of the two form factors for $B \rightarrow D^{(*)}\ell\bar{\nu}$ which at $\omega=1$ are protected from first order corrections in the heavy quark expansion.

vertex	m_c	$b_{A_1}/2$	a_+
original	1.44	1.16	1.11
	1.45	1.12	1.17
exponential	1.55	.95	1.83
	1.50	.97	1.34
	1.44	1.01	1.19
	1.40	1.06	1.17
	1.35	1.15	1.17
	1.30	1.56	1.19

(48)

As we have explained elsewhere [3], the unphysical procedure of changing the quark masses while holding the meson masses fixed can lead to clearly unphysical values for amplitudes. The interesting result in the exponential case is the very large corrections to a_+ for any reasonable value of m_c . Thus our conclusion regarding the existence of large corrections to the heavy-quark limit in at least one of $B \rightarrow D^*\ell\bar{\nu}$ or $B \rightarrow D\ell\bar{\nu}$ [2] remains unchanged.

Conclusions

We have thoroughly explored a relativistic quark model for hadrons containing one heavy quark. It is extremely economical in its description of nonperturbative QCD, its only parameters being the quark masses, yet it is consistent with the symmetries of QCD. It displays

overall agreement, across a broad range of different processes, with the data when it exists and with more complicated models such as QCD sum rules in the absence of data. The main difference with other models is the suggestion that large nonperturbative departures from the heavy quark limit occur in certain quantities, most notably in the processes $B \rightarrow D^{(*)}\ell\nu$ and in the heavy-quark contribution to the $DD^*\gamma$ coupling. At the same time, it is consistent with data for the shape of the spectrum for $B \rightarrow D^*\ell\nu$ and for the branching ratios for $D^* \rightarrow D\gamma$. To test the pattern of deviations from the heavy-quark limit in our model and others, we especially encourage efforts to extract and compare V_{cb} from each of $B \rightarrow D^*\ell\nu$, $B \rightarrow D\ell\nu$ and $\Lambda_b \rightarrow \Lambda_c\ell\nu$.

Acknowledgements

R.L. thanks M. Clayton for helpful comments and B.H. thanks M. Luke for discussions. This research was supported in part by the Natural Sciences and Engineering Research Council of Canada.

References

- [1] B. Holdom and M. Sutherland, Phys. Rev. D **47**, 5067 (1993).
- [2] B. Holdom and M. Sutherland, Phys. Lett B **313**, 447 (1993).
- [3] B. Holdom and M. Sutherland, Phys. Rev. D **48**, 5196 (1993).
- [4] B. Holdom and M. Sutherland, Phys. Rev. D **49**, 2356 (1994).
- [5] B. Holdom, M. Sutherland and J. Mureika, Phys. Rev. D **49**, 2359 (1994).
- [6] M. Sutherland, Z. Phys. C **63**, 111 (1994).
- [7] M. Neubert, V. Rieckert: Nucl. Phys. B 382, 97 (1992); M. Neubert: SLAC Report No. SLAC-PUB-6263, 1993 (to be published in Phys. Rep.).
- [8] B. Holdom and M. Sutherland, University of Toronto report No. UTPT-94-07, hep-ph/9403228, 1994 (to be published in Z. Phys. C).
- [9] CLEO Collaboration, P. Avery et al., Cornell report No. CLNS 94/1280, CLEO 94-10, hep-ph/9403359, unpublished (1994).
- [10] *Review of Particle Properties*, Phys. Rev. D 50, 1173 (1994).
- [11] J.F. Amundson et al., Phys. Lett. B **296**, 415 (1992).
- [12] P. Colangelo, F. De Fazio and G. Nardulli, I.N.F.N. report No. BARI-TH/94-180, hep-ph/9406320, unpublished (1994).
- [13] P. Colangelo *et al.*, preprint UGVA-DPT 1994/06-856, BARI-TH/94-171, hep-ph/9406295, unpublished (1994).

- [14] W.A. Bardeen and C.T. Hill, Phys. Rev. D **49**, 409 (1994).
- [15] L. Randall and E. Sather, Phys. Lett. B **303**, 345 (1993).
- [16] E. Jenkins and M.J. Savage, Phys. Lett. B **281**, 331 (1992).
- [17] CLEO Collaboration, P. Avery et al., Phys. Lett. B **331**, 236-244 (1994).
- [18] A.F. Falk, Nucl. Phys. **B378**, 79 (1992).
- [19] D. Scora, University of Toronto Ph.D. thesis, unpublished (1994).
- [20] P. Colangelo, G. Nardulli, A.A. Ovchinnikov and N. Paver, Phys. Lett. B **269**, 201 (1991).
- [21] P. Colangelo, G. Nardulli and N. Paver, Phys. Lett. B **293**, 207 (1992).
- [22] T.B. Suzuki, T. Ito, S. Sawada and M. Matsuda, Nagoya University report No. DPNU-93-35, Aichi University report No. AUE-04-93, unpublished (1993).
- [23] N. Isgur and M.B. Wise, Phys. Rev. D **43**, 819 (1991).
- [24] Y.-B. Dai, C.-S. Huang and H.-Y. Jin, Z. Phys. C **60**, 527 (1993).
- [25] F.E. Close and A. Wambach, RAL-94-041, hep-ph/405314.
- [26] T. Huang and C.-W. Luo, BIHEP-TH-94-35, hep-ph/9409277.
- [27] C. Bernard, Y. Shen and A. Soni, Phys. Lett. **317B**, 164 (1993); UKQCD Collaboration, Phys. Rev. Lett. **72**, 462 (1994).
- [28] E. Jenkins and M.J. Savage, Phys. Lett. B **281**, 331 (1992).

Figure captions

FIG. 1: Comparison of model prediction for $B \rightarrow D^* \ell \bar{\nu}$ with recent CLEO data [9]. The notation is the same as in [9].

FIG. 2: Full-model form factors c_i and d_i , defined in (29) and (30). Certain coefficients have been divided out as explained in the text. Also shown is the Isgur-Wise function $\tau_{1/2}$, defined in (31).

FIG. 3: Full-model form factors f_i and g_i , defined in (29) and (30). Certain coefficients have been divided out as explained in the text. Also shown is the Isgur-Wise function $\tau_{3/2}$, defined in (31).

FIG. 4: Full-model form factors h_i and k_i , defined in (29) and (30). Certain coefficients have been divided out as explained in the text. Also shown is the Isgur-Wise function $\xi_{3/2}$, defined in (31).

FIG. 5: Full-model form factors for $B \rightarrow D \ell \nu$. a_{\pm} are for the ground-state D , and l_{\pm} are for its first radial excitation, as defined in (29) and (30).

FIG. 6: Electron energy spectra for resonant semileptonic B decays in the full model.

FIG. 7: Electron energy spectra for resonant semileptonic B decays to excited D states only.

FIG. 8: Differential spectrum for $B \rightarrow 1 \ 1_{1/2}^+ \ell \nu$. Normalization is such that the spectrum becomes equal to the Isgur-Wise function $\tau_{1/2}$ when the form factors are replaced by their values in the heavy-quark limit.

FIG. 9: Differential spectrum for $B \rightarrow 1 \ 1_{3/2}^+ \ell \nu$. Normalization is such that the spectrum becomes equal to the Isgur-Wise function $\tau_{3/2}$ when the form factors are replaced by their values in the heavy-quark limit.

FIG. 10: Comparison of usual damping factor with exponential damping factor for B meson, with physical values of parameters.

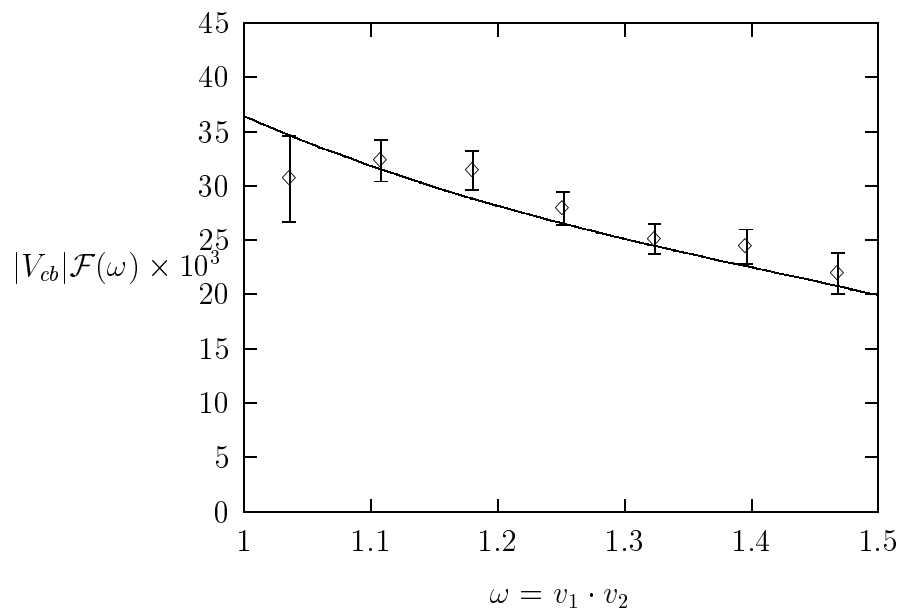


Figure 1

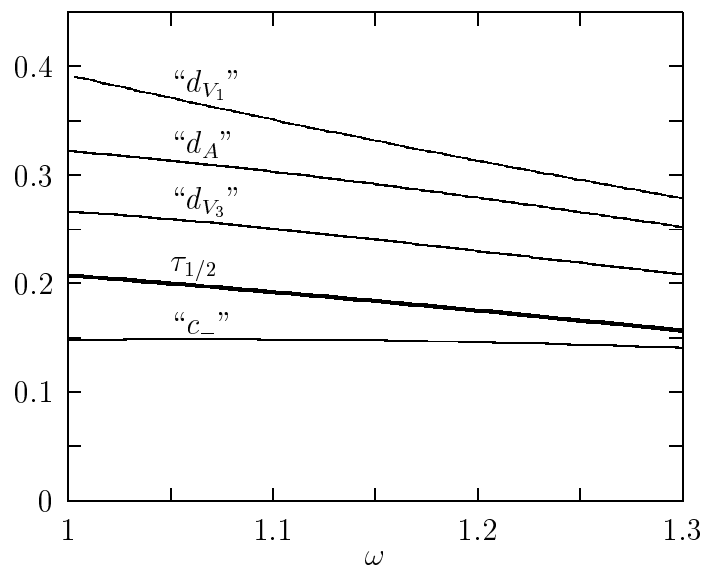


Figure 2

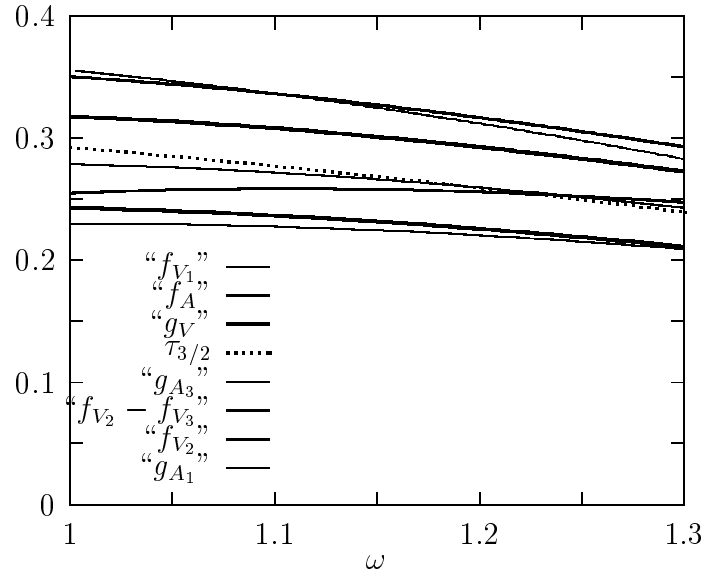


Figure 3

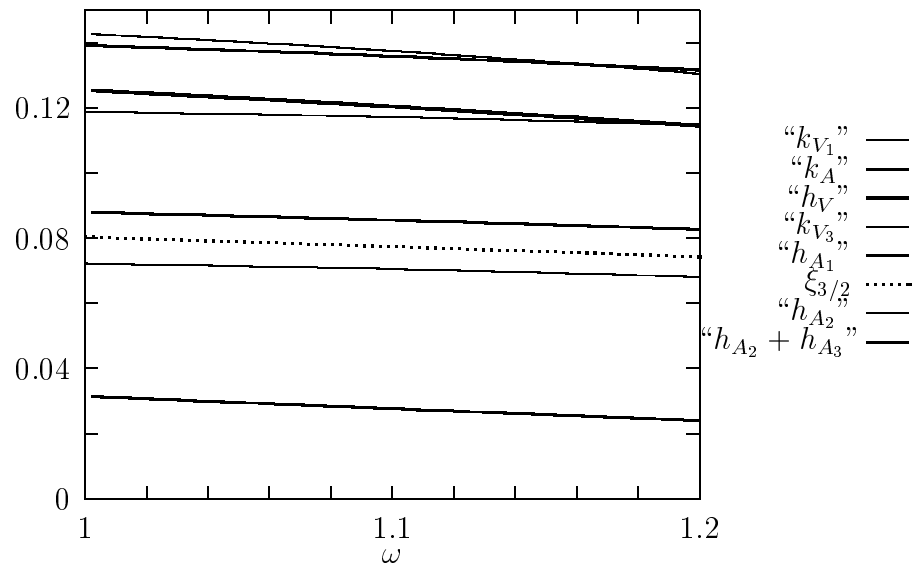


Figure 4

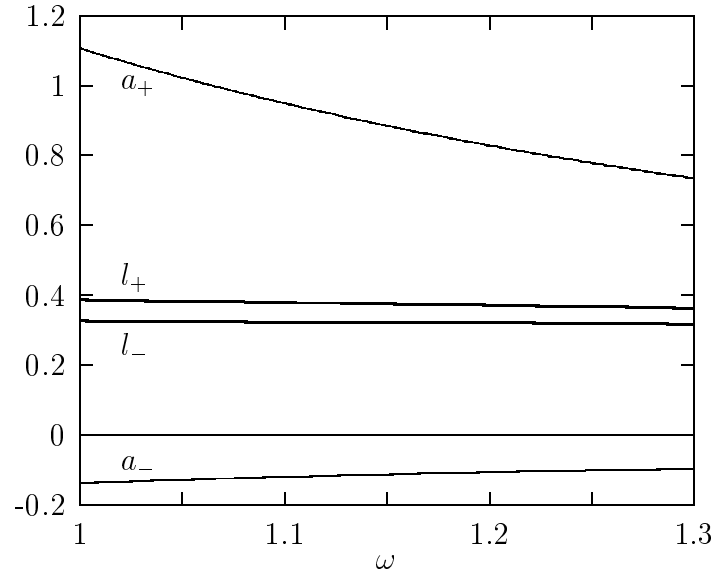


Figure 5

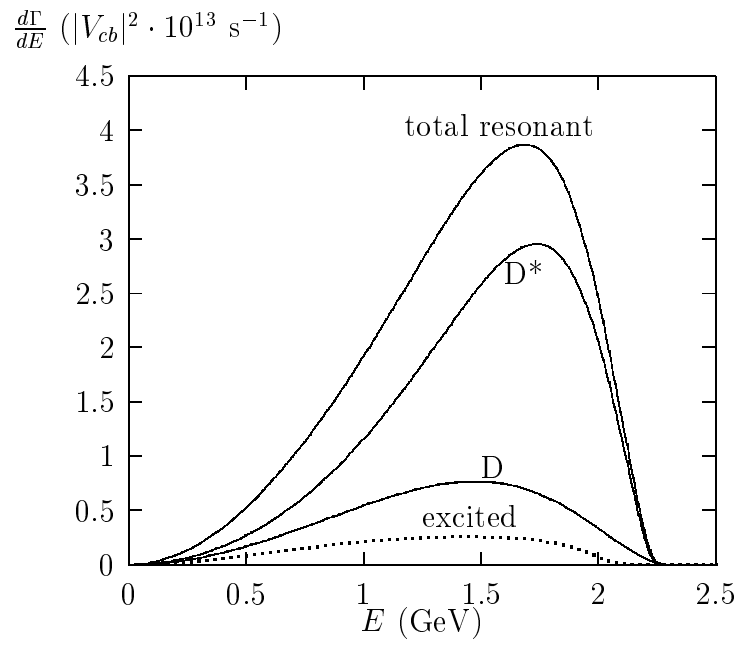


Figure 6

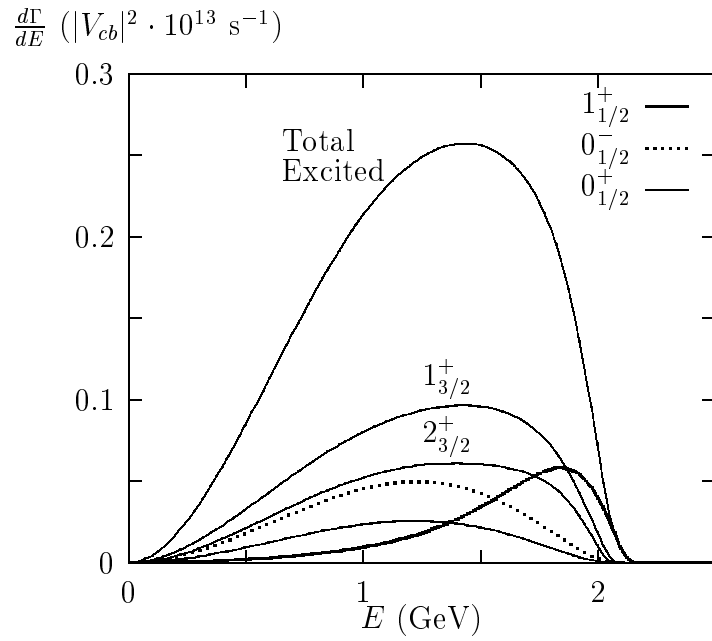


Figure 7

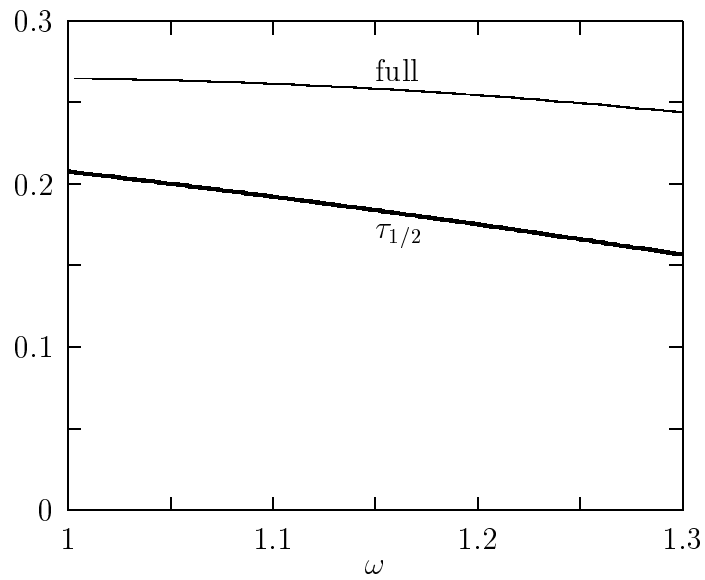


Figure 8

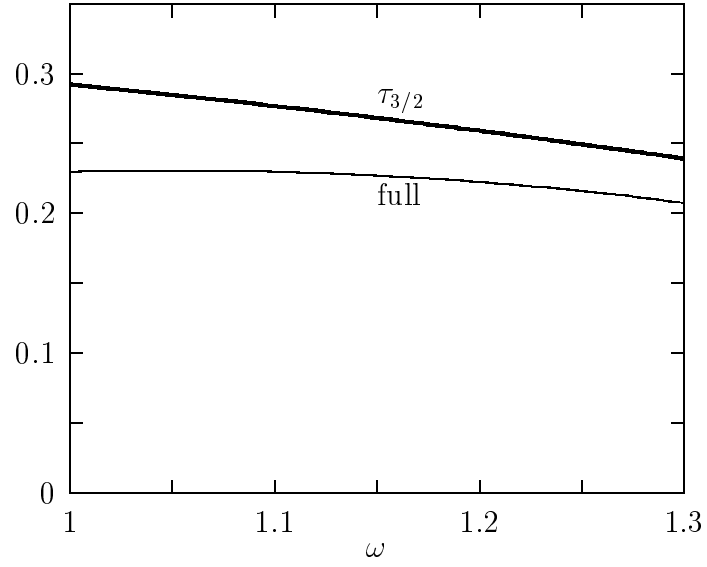


Figure 9

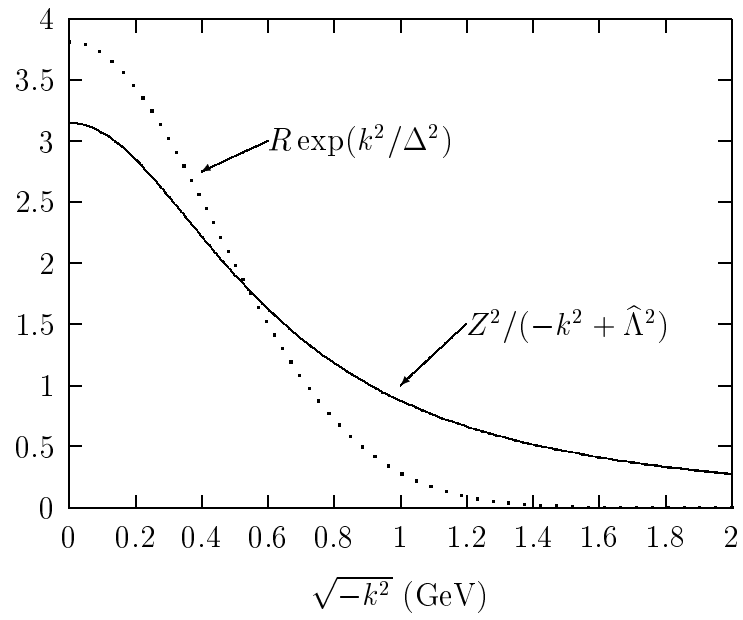


Figure 10

This figure "fig1-1.png" is available in "png" format from:

<http://arxiv.org/ps/hep-ph/9410324v1>

This figure "fig1-2.png" is available in "png" format from:

<http://arxiv.org/ps/hep-ph/9410324v1>

This figure "fig1-3.png" is available in "png" format from:

<http://arxiv.org/ps/hep-ph/9410324v1>

This figure "fig1-4.png" is available in "png" format from:

<http://arxiv.org/ps/hep-ph/9410324v1>

This figure "fig1-5.png" is available in "png" format from:

<http://arxiv.org/ps/hep-ph/9410324v1>